## SHEAR DEFORMATION CHARACTERISTICS

To investigate shear deformation characteristics of each deposit layer, behavior of horizontal displacement of ring frames composing one layer (cf. Table 1) is considered. Horizontal displacement for a layer is calculated by the difference of displacements at the top and bottom of a concerned layer obtained from displacement transducers. When horizontal displacement is divided by the height of the layer, shear strain, $\gamma$, of the layer can be obtained. On the other hand, since horizontal force is unable to be directly captured, horizontal acceleration measured with accelerometers is used to evaluate deformation characteristics in this paper. Acceleration can be one of the reference properties defining horizontal force or stress relating shear deformation.

Figure 12 shows examples of the relationship between $\gamma$ and horizontal acceleration. Here horizontal acceleration, $a$, is the mean value of the horizontal accelerations at the top and bottom of a concerned layer. The relationships shown in the figure look scattered and are not so uniform due to the input motion based on seismic ground motion containing various frequency components. However, these have some correlation with a gradient of loops, which is similar to a stress-strain loop in cyclic shear. In addition, little residual deformation after shaking are observed.

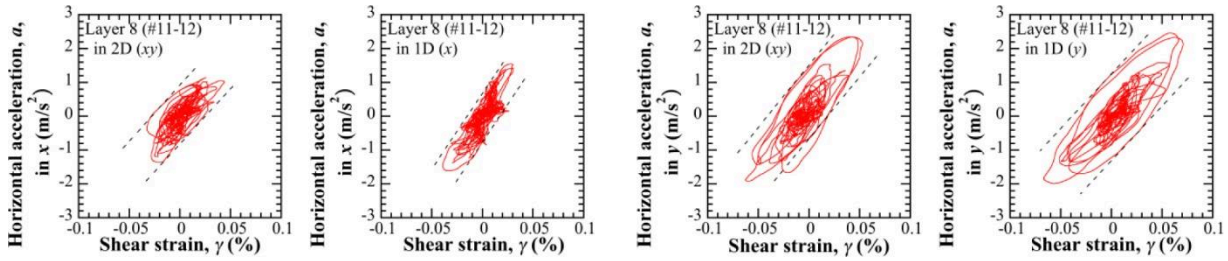


**Figure 12. Relationship between shear strain and horizontal acceleration of Layer No.8 in 2-D and 1-D ($x$ and $y$) shaking cases.**

To evaluate the correlation between $\gamma$ and $a$, strain-acceleration loops at 0.4-second intervals are drawn and their representative gradient is assumed, as shown in Figure 13 for example. To eliminate an arbitrary decision, the gradient of a loop, $C$, is defined as the following:

$$C = \frac{\Delta a}{\Delta \gamma} = \frac{a_{\max} - a_{\min}}{\gamma_{\max} - \gamma_{\min}}$$

where $\Delta\gamma$ and $\Delta a$ are the amplitudes of $\gamma$ and $a$, $\gamma_{\max}$ and $\gamma_{\min}$ are the maximum and minimum values of $\gamma$, and $a_{\max}$ and $a_{\min}$ are the maximum and minimum values of $a$ with respect to the loops with time duration of 0.4 seconds in the figure. After such process, $C$ is obtained as shown in Figure 14 with the cyclic shear strain amplitude, $\gamma_c$, defined as the following:

$$\gamma_c = \frac{|\gamma_{\max}| + |\gamma_{\min}|}{2}$$

In this figure, to avoid influence of height and volume of the layer, only $C$ of Layers Nos.5-8 are considered because the heights of these layers are the same. In addition, scattered or indistinct loops are excluded. Similar to the shear-modulus reduction curve in small and small-to-medium shear strain domains, the coefficient tends to decrease with $\gamma_c$ increase. The difference between $C$ of 1-D and 2-D shaking is not clear from the figure, but it seems that $C$ of 1-D shaking tends to be located relatively above $C$ of 2-D shaking, especially in the $x$ direction. This tendency may correspond to that of the acceleration and displacement responses in the 1-D

shaking to be greater than those in the 2-D shaking. Since force can be obtained by multiplying acceleration by mass, such relationship between $\gamma$ and $a$ can be useful information to evaluate shear deformation characteristics.

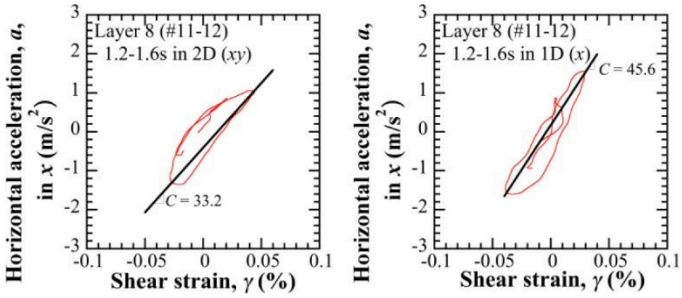


**Figure 13. Determination of the representative gradient of a cyclic loop: Loops and their gradients in the *x* direction of Layer No.8 between 1.2-1.6 seconds in 2-D and 1-D (*x*-directional) shaking cases.**

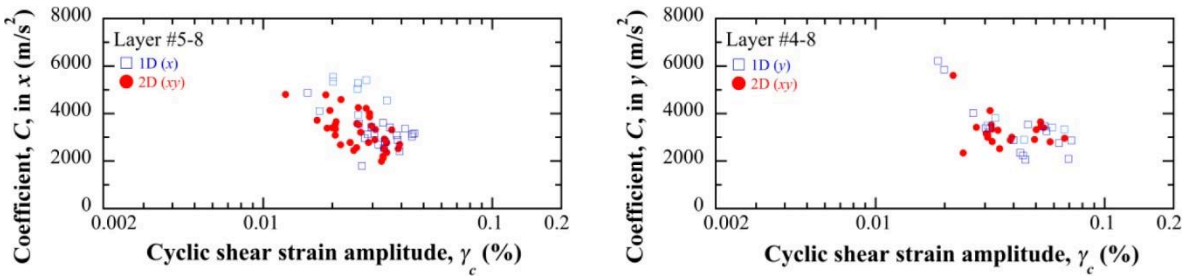


**Figure 14. Coefficients of cyclic loop gradient with cyclic shear strain amplitude obtained from Layers Nos.5-8.**

## CONCLUSION

In order to examine the cyclic behavior of deposits under horizontal one-dimensional (one-directional; *x*- or *y*-directional) and two-dimensional (multi-directional in the *x*-*y* plane) seismic ground motion in the domain of small shear deformation, the results obtained from the E-Defense shaking tests on a large-scale specimen of a non-liquefiable dry sand deposit prepared in a shear box are investigated. Based on the observation of the cyclic behavior obtained from accelerometers in the deposit and accelerometers and displacement transducers on frames of the shear box, it can be recognized that the acceleration and displacement responses of the deposit in 1-D shaking are larger than those in 2-D shaking when the input motions of 1-D and 2-D shaking in each (*x*- or *y*-) direction are practically similar. In addition, to evaluate shear deformation characteristics of deposit layers, the relationship between shear strain and horizontal acceleration of each layer is presented as a cyclic loop. It can be seen that the loop gradients tend to decrease with increase of shear strain, and the difference between the gradients in 1-D and 2-D shaking cannot be clearly identified through these tests.

## REFERENCES

Enokida, R. and Kajiwara, K. (2017). "Nonlinear signal-based control with an error feedback action for nonlinear substructuring control." *Journal of Sound and Vibration*, 386(6), 21-37.

Fukutake, K. and Matsuoka, H. (1989). "A unified law for dilatancy under multi-directional simple shearing." *Journal of Geotechnical Enginering*, Japan Society of Civil Engineers,

412(III-12), 143-151 (in Japanese).
Ishihara, K. and Yamazaki, F. (1980). "Cyclic simple shear tests on saturated sand in multi-directional loading." *Soils and Foundations*, 20(1), 45-59.
Matsuda, H., Sakuradani, K. and Emoto, N. (2000). "Effects of earthquake-induced settlement of clay layer on the ground subsidence." *Proc. 12th World Conference on Earthquake Engineering*, Paper No.1097.
Suzuki, H., Tokimatsu, K. and Tabata, K. (2014). "Factors affecting stress distribution of a 3x3 pile group in dry sand based on three-dimensional large shaking table tests." *Soils and Foundations*, 54(4), 699-712.
Tabata, K. and Sato, M. (2010). "E-Defense shaking table tests on the behavior of a pile-foundation structure in large-scale model ground under multi-dimensional motions." *Proc. 9th U.S, National and 10th Canadian Conf. on Earthquake Engineering*, Toronto, Canada, 6919-6928.
Yasuda, S. (1988). *From investigations to remedial measures for liquefaction*. Kajima Institute Publishing (in Japanese).

# Cyclic Behavior of Low-Plasticity Fine-Grained Soils with Varying Pore-Fluid Salinity

Mohammad M. Eslami, Ph.D., S.M.ASCE[1]; Scott J. Brandenberg, Ph.D., P.E., M.ASCE[2]; and Jonathan P. Stewart, Ph.D., P.E., F.ASCE[3]

[1]Postdoctoral Scholar, Dept. of Civil and Environmental Engineering, Univ. of California, Los Angeles, CA 90095. E-mail: mandro@ucla.edu
[2]Professor, Dept. of Civil and Environmental Engineering, Univ. of California, Los Angeles, CA 90095. E-mail: sjbrandenberg@ucla.edu
[3]Professor and Chair, Dept. of Civil and Environmental Engineering, Univ. of California, Los Angeles, CA 90095. E-mail: jstewart@seas.ucla.edu

## ABSTRACT

A series of cyclic and monotonic direct simple shear experiments was conducted on mixtures of non-plastic silt and bentonite, prepared with two different pore fluids: fresh deionized water, and saline-water with a 35 g/L concentration of NaCl (consistent with sea water). The clay fractions were adjusted to achieve a plasticity index of PI=9, with the fresh-water blend requiring 5% bentonite and the saline water blend requiring 10% bentonite. Though both blends have the same plasticity index, differences in cyclic behavior were observed. The relationship of cyclic stress ratio versus number of cycles and the ratio of cyclic stress to monotonic undrained strength was higher for the saline water blend than for the fresh water blend. Results indicate that plasticity index alone is an insufficient indicator of cyclic strength. Corrections for pore fluid chemistry (and by extension, depositional environment) may be necessary, in addition to possibly other factors, for procedures to assess the potential for liquefaction susceptibility and cyclic softening.

## INTRODUCTION

The essential first step in characterizing seismic soil behavior is to assess liquefaction susceptibility, where the potential for soil to experience strength loss based on its composition is evaluated. This practice is commonly based on soil index properties such as liquid limit (LL) and plasticity index (PI), and particle size. The “Chinese criteria” by Wang (1979) and its modified version by Seed and Idriss (1982) were among the very first criteria established based on observations of field performance at sites that did and did not “liquefy” in the Haicheng and Tangshan earthquakes in China. Following site reconnaissance of the 1989 Loma Prieta, 1994 Northridge, 1999 Kocaeli and Chi-Chi earthquake events, the Chinese criteria was proven to be unreliable [e.g. Boulanger et al. (1998), and Sancio et al. (2002)] and updated criteria for liquefaction susceptibility were proposed. Andrews and Martin (2000) and Seed et al. (2003) modified the liquid limit and clay fraction required for a fine-grained soil to be considered susceptible to liquefaction but kept the basic Chinese criteria framework in place.

An alternative approach to procedures based on index properties is to perform cyclic laboratory testing to develop liquefaction susceptibility criteria. Following extensive laboratory testing of soils from Adapazari, Bray and Sancio (2006) conclude that soils with PI < 12 with a ratio of natural water content ($w_n$) to LL greater than 0.85 are susceptible to liquefaction, soils with 12 < PI < 18 and $w_n$/LL > 0.8 are moderately susceptible, and soil is otherwise not susceptible. Based on testing of a variety of soils from California, including soil mixtures,

Boulanger and Idriss (2006) suggested that sand-like behavior is likely for PI < 4, whereas clay-like behavior is expected for PI ≥ 7, with a transition zone from sand-like to clay-like behavior for 4 < PI < 7. Cyclic strength of clay-like soil normalized by monotonic undrained shear strength is represented as a function of plasticity index and earthquake magnitude in their study. It is unclear the extent to which differences between the Bray and Sancio (2006) approach and the Boulanger and Idriss (2006) approach are due to differences in the soils comprising their respective datasets. The soils tested by Bray and Sancio (2006) were overbank deposits of the Sakarya and Çark River, whereas the soils tested in the Boulanger and Idriss (2006) study were predominantly marine clays. Both studies agree that cyclic laboratory testing is the recommended approach, with empirical relationships reserved for projects where such testing is infeasible [e.g. Boulanger and Idriss (2007); Chu et al. 2008].

Additional studies since 2006 have demonstrated the limitations of PI for categorizing the cyclic response of soils. A recent study by Jang and Santamarina (2016) highlight that soil plasticity depends on pore-fluid chemistry in addition to minerology. Gratchev et al. (2006) have criticized the effectiveness of plasticity index as a measure for liquefaction susceptibility potential when the pore-fluid contains high concentrations of ions and argued that clay mineralogy and pore-fluid chemistry play an important role. Moreover, effects of changes in pH levels and varying pore-fluids have been shown to influence cyclic resistance of natural soils [e.g. Gratchev and Sassa (2009, 2013)]. Ajmera et al. (2015) recognized substantial differences in cyclic response of quartz-montmorillonite versus quartz-Kaolinite mixtures (both at PI = 14). Ajmera et al. (2016) found that fewer loading cycles were required to reach from 2.5% to 10% double amplitude shear strains in the quartz-kaolinite mixtures compared to quartz-montmorillonite.

This paper discusses the effects of pore fluid salinity on cyclic response of low-plasticity fine-grained mixtures. Details of the mineral blends and pore fluids are presented first, followed by a description of the laboratory test program, which consisted of monotonic and cyclic constant-height direct simple shear tests, consolidation tests, and Atterberg limits tests. The results are then synthesized and compared with previous findings from the literature.

## SOIL MIXTURES USED IN EXPERIMENTAL STUDY

Two mixtures of commercial non-plastic silt (rock powder) and bentonite were prepared at PI = 9. To inspect the effects of the pore-fluid chemistry on cyclic behavior, the mixtures were either blended with deionized fresh water or saline water with a concentration of 35g/L of NaCL (approximate concentration of sea water). Properties of the mixtures as well as their constituent minerals are summarized in Table 1. The ID of each mixture is based on its constituents; (S) Silt, (B) Bentonite, (FW) Fresh water, and (SW) Saline Water. These mixtures plot on top of each other and slightly above the A-line on Casagrande's plasticity chart, classifying as low-plasticity clay (CL) per the Unified Soil Classification System (USCS). Note from Table 1 that the mixtures have essentially identical values of LL, PL and PI, and are therefore indistinguishable based on plasticity alone.

Mixtures were first made as a slurry above their liquid limits, then transferred to acrylic tubes with a dimeter of 72.4mm, slightly larger than the simple shear specimens. The slurries were consolidated inside the tubes to a vertical consolidation stress of about 35 kPa and were subsequently extruded from the acrylic tubes and trimmed to reach the diameter (66mm) and height of 28mm (1.1 inch) desired for cyclic or monotonic shearing. The specimens were then placed inside a wire-reinforced latex membrane and mounted in the simple shear device. They

were then further consolidated to the desired vertical pressure and overconsolidation ratio before being sheared. The vertical consolidation stress was always higher than the pre-consolidation pressure applied in the acrylic tube, thereby ensuring the specimens are normally consolidated and reducing effects of sample disturbance (e.g., Ladd 1991).

**Table 1. Properties of mixtures used in experimental program**

| *ID* | *% Silt*[a] | *% Bentonite*[b] | *Pore-fluid* | $G_s$ | *LL* | *PL* | *PI* |
|---|---|---|---|---|---|---|---|
| *SBFW* | 95 | 5 | Fresh water | 2.64 | 31.2 | 22.6 | 8.6 |
| *SBSW* | 90 | 10 | Saline water | 2.67 | 31.9 | 23.1 | 8.8 |

[a] Sil-co-sil #45 ground silica, Non-plastic
[b] *LL* = 455.3, *PL* = 39.6, *PI* = 415.7

## CONSOLIDATION BEHAVIOR

One dimensional consolidation tests were performed on the blends following the procedures described in ASTM D2435. Results of incremental load consolidation tests are presented in Figure 1, where compression properties of the mixtures are shown. $C_c$, $C_r$, and $C_\alpha$ are the virgin compression, recompression, and secondary compression indices, respectively. Values of $c_v$ and $k$ are obtained based on Taylor's method (1948) and plotted for loading stages where a good measure of the time to end of primary consolidation could be made. The logarithm of permeability of soil has been observed to be linearly proportional to void ratio, with the slope defined as $C_k = \Delta e / \Delta \log k$ [Fox (1999)]. Results indicate that the SBFW and SBSW blends have generally similar compression properties.

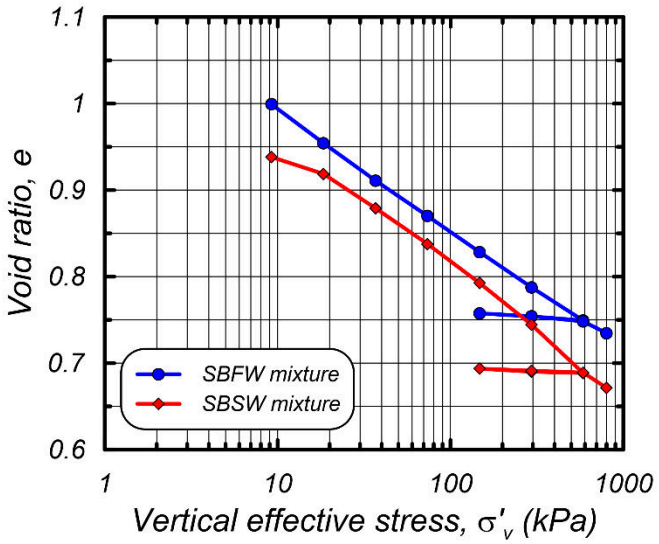


| *Mixture* | $C_c$ | $C_r$ | $C_k$ | $C_\alpha$ |
|---|---|---|---|---|
| *SBFW* | 0.138 | 0.014 | 0.089 | 0.011 |
| *SBSW* | 0.145 | 0.008 | 0.079 | 0.008 |

**Figure 1. Oedometer test results of SBFW and SBSW mixtures**

## MONOTONIC SHEAR RESPONSE

Constant-height direct simple shear (DSS) tests were conducted on specimens extruded from the acrylic tubes and trimmed to a diameter of 66mm and initial height of 28mm. The UCLA Bi-directional Broadband Simple Shear (BB-SS) apparatus (Shafiee et al., 2017) was used for shearing the specimens. The device is configured for both stress-controlled and strain-controlled constant height loading over a wide frequency range. Further details on the testing procedures

can be found in Eslami (2017).

Strain-controlled monotonic shearing tests were performed with a strain rate of about 1%/min and a duration of 24 minutes. These tests were conducted at an initial vertical consolidation pressure of $\sigma'_{vc}$ = 50 kPa. Some specimens were overconsolidated to a maximum vertical pressure of $\sigma'_{vc,max}$ before being unloaded to $\sigma'_{vc}$. Secondary compression occurred during consolidation of the soil, rendering an overconsolidation ratio that is larger than the mechanical preload ratio $\sigma'_{vc,max}/\sigma'_{vc}$. Overconsolidation ratio, OCR, was computed based on distance to the normal consolidation line rather than being taken as equal to the preload ratio to account for the influence of secondary compression. Figure 2 represents results of constant-height monotonic shear tests on the two soil mixtures in normalized stress space. The normally consolidated specimens exhibit nearly perfectly plastic ductile behavior and are generally contractive, whereas the overconsolidated specimens show a stress-strain response with some strain softening at higher strains. The overconsolidated specimens exhibit dilative behavior up to a peak shear stress (at about 4% shear strain) and then transition to contractive behavior.

The undrained strength is chosen based on the peak shear resistance of each specimen, and Figure 2 shows that the SBSW mixture consistently exhibits higher normalized undrained strength ratios ($s_u/\sigma'_{vc}$). Combinations of the final void ratio of each specimen and the vertical effective stress at a peak undrained shear strength were observed to provide linear fits that were parallel to the normal consolidation line, indicating that the undrained shear strengths for these mixtures normalizes with effective consolidation stress and OCR (clay-like behavior). Note that a true critical state was not reached during the monotonic shearing tests and therefore critical state lines could not be obtained.

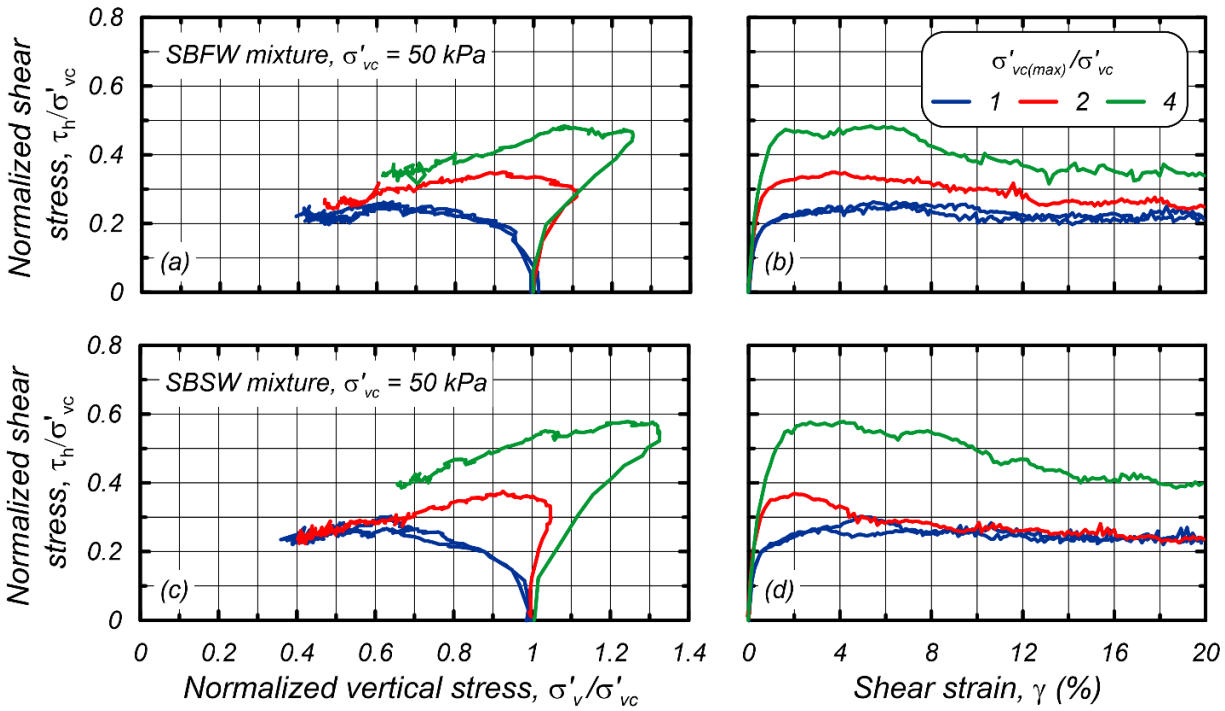


**Figure 2. Constant-height monotonic DSS response of mixtures. Stress-paths and stress-strain curves; (a) and (b): SBFW, (c) and (d): SBSW**

Undrained shear strength ratios in the form given by Ladd (1991) are shown in Figure 3 for both mixtures. The average normally consolidated undrained shear strength ratio for the two

mixtures (0.213 and 0.229) and exponents for the OCR terms are in the range reported in Ladd (1991) for sedimentary clays.

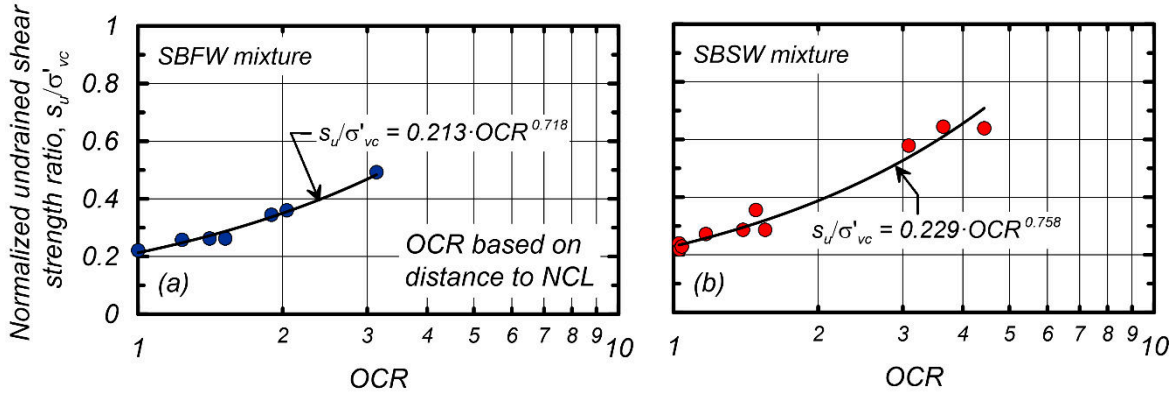


**Figure 3. Normalized undrained shear strength ratio vs. OCR relationships; (a) SBFW, and (b) SBSW**

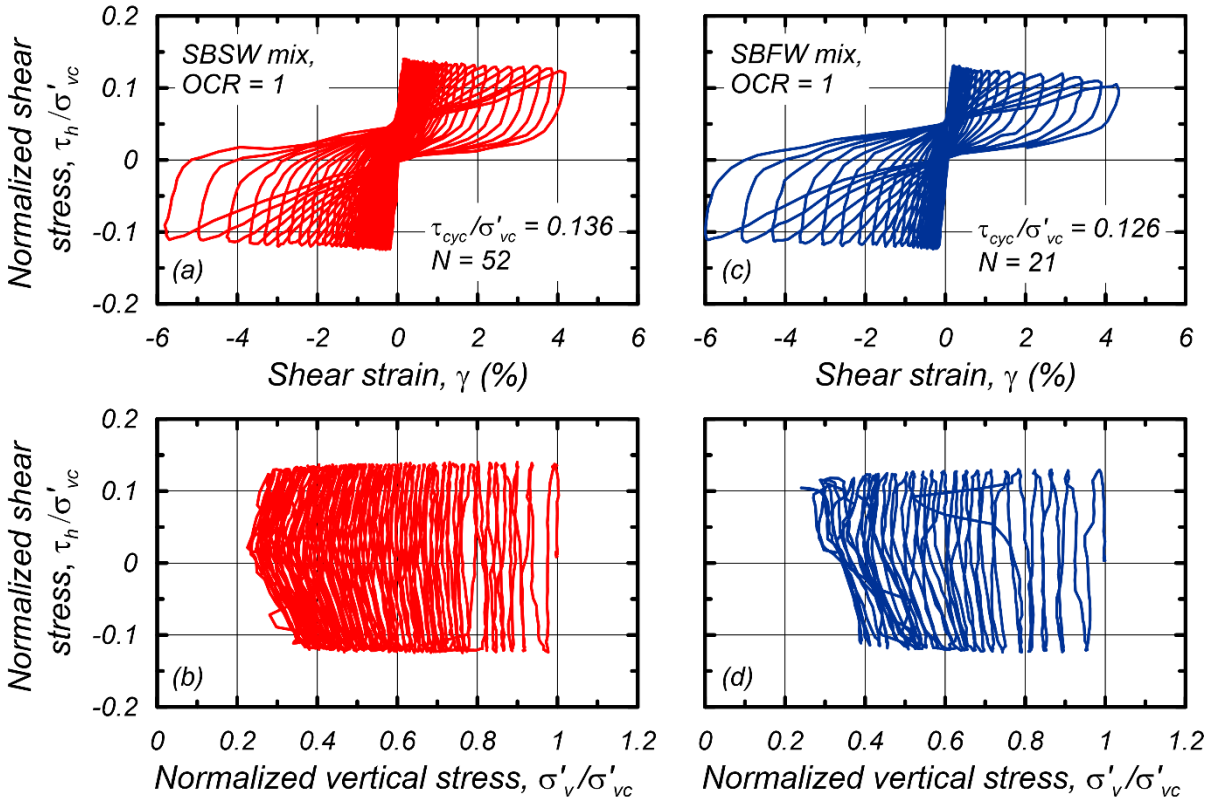


**Figure 4. Typical stress-strain and stress-path response of constant-height DSS cyclic shear; (a) and (b): SBSW, (c) and (d): SBFW**

## CYCLIC SHEAR RESPONSE

Cyclic stress-controlled constant-height DSS tests were performed on normally consolidated specimens of the two mixtures at a vertical effective stress of 50 kPa. Uniform sinusoidal cyclic stress ratios with frequency of 0.1Hz were applied to the specimens. Figure 4 presents typical stress-strain and stress-path response of normally consolidated specimens for the two mixtures.

The applied cyclic stress ratios as well as the number of uniform cycles to reach a peak shear strain of 3% are marked inside the plots. Generally, both mixtures produce wide hysteresis loops similar to that of clay-like type of soils and don't reach to a vertical effective stress of zero at large strains. Though the applied CSR ($\tau_{cyc}/\sigma'_{vc}$) in Figure 4 (a) and (c) are relatively close, SBSW reaches a peak shear strain of 3% in 52 cycles, whereas the SBFW mixture reaches the same peak shear strain in 21 cycles. This is significant difference between the cyclic responses of the two mixtures, despite them having the same PI and cyclic testing protocol. Maximum equivalent excess pore pressure ratios ( $r_u = 1 - \frac{\sigma'_v}{\sigma'_{vc}}$ ) for the tests shown in Figure 4 at 10% shear strain are 0.78 and 0.84 for the SBFW and SBSW mixtures, respectively. The SBFW mixture accumulates shear strains more rapidly than the SBSW mixture.

## CYCLIC STRENGTHS AND INFLUENCE OF PORE-FLUID SALINITY

Figure 5 (a) presents the ratio of cyclic stresses normalized with effective consolidation stress ($\tau_{cyc}/\sigma'_{vc}$) versus number of uniform loading cycles to reach a peak shear strain of 3% for normally consolidated specimens of the two mixtures. The plot also shows least squares regressed power functions in the form given in equation (1), where the cyclic resistance ratio (CRR) is related to the number of uniform cycles (N) to reach the 3% shear strain failure criteria.

$$CRR = a \cdot N^{-b} \quad (1)$$

Fitting parameters *a* and *b*, shown in Figure 5a, are in the common range provided in the literature for natural clays and mine tailings, as reported by Boulanger and Idriss (2007). The SBSW mixture exhibits higher CRR for a given number of loading cycles compared to the SBFW blend. For example, at N = 30, the CRR is 0.138 and 0.126 for the SBSW and SBFW mixtures, respectively. Furthermore, Figure 5 (b) provides plots of the cyclic stress normalized by the monotonic undrained shear strength of the mixtures ($\tau_{cyc}/s_u$), where the undrained shear strength is computed based on normalized monotonic strength relationships provided in Figure 3 (a) and (b). The two blends have essentially identical $\tau_{cyc}/s_u$ relationships. For instance, at N = 30, the cyclic stress to reach a peak shear strain of 3% is equal to 0.60 for both blends. This trend occurs because the SBFW blend has a lower monotonic undrained strength ratio.

Boulanger and Idriss (2007) recommend $\tau_{cyc}/s_u = 0.83$ for normally consolidated clay-like materials with PI > 7 and N = 30. This recommendation is considerably higher than values observed for the mineral blends in Fig. 5, for which $\tau_{cyc}/s_u = 0.60$. The lower values obtained in the current study are consistent with other experimental studies that have investigated mixtures prepared in the laboratory [e.g. Price et al. (2015), Reid and Fourie (2017), and Soysa and Wijewickreme (2017)] whereas the recommendations in Boulanger and Idriss (2007) are based on experiments on naturally deposited soils and mine tailings that are older and perhaps have more complex mineralogical composition compared to blends of two minerals consolidated for just a few days in the laboratory.

## CONCLUSIONS

A series of cyclic and monotonic direct simple shear experiments was conducted on two low-plasticity fine-grained mixtures of non-plastic silt with bentonite clay minerals blended with fresh deionized water or saline water. Though both blends have the same plasticity index PI = 9, differences in the monotonic and cyclic responses were observed. This indicates that plasticity

characteristics are an insufficient indicator of the cyclic strength of fine-grained soils, and that pore fluid chemistry and mineralogy plays an additional role.

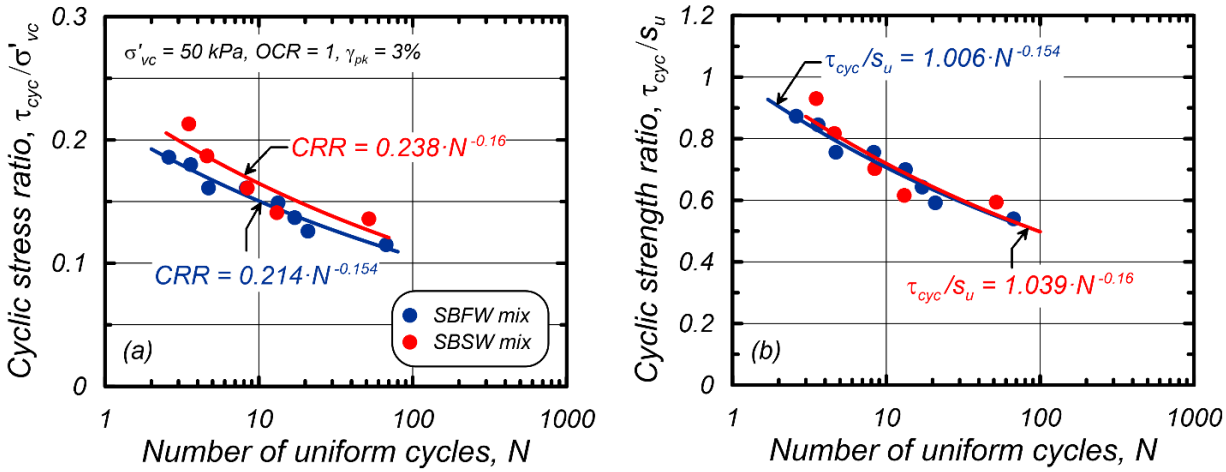


**Figure 5. Cyclic strengths for normally consolidated specimens to reach 3% peak shear strain; (a) cyclic stress ratios ($\tau_{cyc}/\sigma'_{vc}$) versus number of uniform loading cycles, and (b) cyclic strength ratios ($\tau_{cyc}/s_u$) versus number of uniform loading cycles**

Although the cyclic resistance ratios were different for the two blends, the ratio of cyclic strength to monotonic undrained strength was essentially the same. However, the cyclic strength ratio was lower than empirical relationships recommended by Boulanger and Idriss (2007) for natural soils. Future laboratory tests will explore the influence of overconsolidation ratio on the cyclic strength of the mineral blends presented herein.

## ACKNOWLEDGMENTS

Financial support for this work was provided by the National Science Foundation under award number CMMI-1563638. This support is gratefully acknowledged. The authors thank undergraduate students at UCLA; Ariel Siegel, Mike Yang Liu and Soheil Kashani for their help with running Atterberg limits, consolidation tests, and creating data visualization tools.

## REFERENCES

Ajmera, B., Brandon, T., Tiwari, B. (2015). "Cyclic strength of clay-like materials." Proc. Of the 6th International Conference on Earthquake Geotechnical Engineering, Christchurch, New Zealand.

Ajmera, B., Tiwari, B., Brandon, T. (2016). "Influence of mineralogy and plasticity on the cyclic and post-cyclic behavior of normally consolidated soils." Geotechnical and Structural Congress 2016, ASCE, Phoenix, AZ.

Andrews, D. C. A., and Martin, G. R. (2000). "Criteria for liquefaction of silty soils." Proc., 12th World Conference on Earthquake Engineering, Auckland, New Zealand.

ASTM (2007). "Annual Book of Standards," Vol. 4.08, Soil and Rock (I): D420 -D5611, and Soil and Rock (II): D5714-latest, ASTM International, West Conshohocken, PA, U.S.

Boulanger, R. W., and Idriss, I. M. (2006). "Liquefaction susceptibility criteria for silts and clays." Journal of Geotechnical and Geoenvironmental Engineering, ASCE, 132(11), 1413-1426.